

# Phase transformation in quenched mesomorphic isotactic polypropylene

Zhi-Gang Wang<sup>a</sup>, Benjamin S. Hsiao<sup>a,\*</sup>, Srivatsan Srinivas<sup>b</sup>, Gary M. Brown<sup>b</sup>, Andy H. Tsou<sup>b</sup>,  
Stephen Z.D. Cheng<sup>c</sup>, Richard S. Stein<sup>d</sup>

<sup>a</sup>Department of Chemistry, State University of New York at Stony Brook, Stony Brook, NY 11794-3400, USA

<sup>b</sup>ExxonMobil Chemical Company, Baytown Polymers Center, Baytown, TX 77522-5200, USA

<sup>c</sup>The Maurice Morton Institute of Polymer Science, University of Akron, Akron, OH 44325-3909 USA

<sup>d</sup>Department of Chemistry, University of Massachusetts, Amherst, MA 01003, USA

Received 2 January 2001; received in revised form 5 April 2001; accepted 13 April 2001

## Abstract

The transformation of mesomorphic phase to  $\alpha$ -monoclinic crystal phase in quenched isotactic polypropylene has been investigated by TEM, DSC and time-resolved SAXS and WAXD methods. It is found that even though the initial appearance of the cluster structure in mesomorphic i-PP seems to support the model of a multi-step process for polymer crystallization, results indicate that the transformation is not spontaneous. In the cluster domains, a significant fraction of chain segments must undergo a reorganization process in order to establish the correct registration of helical hands for crystallization. In addition, a fraction of the ordered chains with correct registration of helical hands should also serve as primary nuclei to initiate crystallization. However, the entire cluster domains should not be considered as ‘precursors’. The growth process via secondary nucleation eventually transforms the cluster structure to the lamellar structure. © 2001 Elsevier Science Ltd. All rights reserved.

**Keywords:** Phase transformation; Mesomorphic;  $\alpha$ -Monoclinic crystal

## 1. Introduction

Recently, several new hypotheses have been proposed to explain the mechanism of the initial stages of crystallization from the polymer melt. These hypotheses challenge the conventional view of crystallization via nucleation and growth processes. For example, one hypothesis suggests that density fluctuations are formed first in the melt, especially through the process of spinodal decomposition, which serve as a precursor to crystallization [1–5]. Another hypothesis, championed by Strobl, but debated by Lotz, Cheng, and Muthukumar, suggests that the initial stages of polymer crystallization involve several multi-step processes passing through intermediate states, i.e. from the melt via mesomorphic and granular crystalline layers to lamellar crystallites [6–9]. From a cursory examination of the supporting data, both hypotheses seem credible. However, detailed investigation of the recent results revealed some fundamental problems related to the interpretation of the data. For example, the primary result supporting the spinodal decomposition hypothesis is based on the appearance of small-angle X-ray scattering (SAXS) before wide-

angle X-ray diffraction (WAXD). Our recent study has shown that SAXS can detect a much lower level of crystallinity ( $\sim 0.1\%$ ) than WAXD ( $\sim 1\%$ ), which leads to some questions about the validity of the spinodal decomposition analysis using the SAXS data collected in the ‘induction’ period [10].

In this article, we also raise some ‘issues’ about the hypothesis of the behavior of multi-step processes for polymers involving the passing through of the intermediate mesomorphic structure during crystallization. Strobl has listed evidences from experiments of syndiotactic polypropylene (s-PP), polyethylene (PE), poly( $\epsilon$ -caprolactone) (PCL) and isotactic polypropylene (i-PP) [11–13]. In this study, we have examined the case of i-PP, as this polymer possesses all the characteristics to support a multi-step process. The most interesting aspect of i-PP is that its chains consist of chirality, which require specific registration of four types of helical hands (left- and right-handed helices as well as ‘up’ and ‘down’ positions concerning the CH<sub>3</sub> group) to form a unit cell structure [14]. The mesophase, which may act as ‘precursor’ to crystallization appears to be evident in the quenched samples, but large molecular reorganization has also been detected during the transformation from mesophase to crystalline phase in this study. This again leads to some questions about the role of molecule

\* Corresponding author. Tel.: +1-516-632-7793; fax: +1-516-632-6518.

E-mail address: bhsiao@notes.cc.sunysb.edu (B.S. Hsiao).

packing in the intermediate structure to initiate polymer crystallization.

When crystallized from the molten state, i-PP chains adopt a  $3_1$  helical conformation. These helical chains can organize into several different spatial arrangements giving rise to three distinct polymorphs:  $\alpha$ -monoclinic,  $\beta$ -hexagonal and  $\gamma$ -orthorhombic forms, depending on the crystallization conditions [15–18]. Among these crystal structures, the  $\alpha$ -form (monoclinic) is the most common one. There is also a ‘mesomorphic’ phase, which can be obtained by rapid quenching of molten i-PP. Natta and Corradini [19] first pointed out that this form had an intermediate degree of ordering between the amorphous phase and the crystalline phase. They categorized it as smectic to indicate the presence of two-dimensional ordering. However, the full evidence for the smectic phase in i-PP has not been documented. The description of the mesophase can be quite confusing in the literature. In addition to the smectic phase [19,20], other investigators described the mesomorphic phase as paracrystalline [21,22], micro-crystallites [23–26] and nano-crystallites [27]. The micro-crystallites have been described to possess hexagonal  $\beta$ -phase (5–10 nm across), monoclinic  $\alpha$ -phase (3–5 nm) [23–27], cubic or tetragonal phase (3 nm) [28]. Guerra et al. [29–31] pointed out that comparison of experimental scattering patterns of mesomorphic i-PP with calculated scattering patterns excluded the possibility of micro-crystallites of  $\alpha$ -monoclinic or  $\beta$ -hexagonal i-PP. In addition, Wunderlich et al. [32] suggested that the term conformationally disordered crystal (condis crystal) was more appropriate for the i-PP mesomorphic form, based on its frozen liquid-like structure.

In our opinion, the more sensible description of the mesomorphic phase in i-PP is that it consists of clusters of ordered helical chain segments with a random assembly of helical hands (left or right) [7]. The average interchain distance can be characterized by the diffraction maximum near the amorphous scattering peak ( $2\theta = 15.7^\circ$ ). The signature of the 3-turn helix in the chains can be identified by the second diffraction maximum at a larger angle ( $2\theta = 20.6^\circ$ ). As a result, a characteristic of the quenched mesomorphic form is the appearance of two broad, diffuse peaks in the wide-angle X-ray diffraction (WAXD) pattern.

## 2. Experimental

In this study, the i-PP sample was supplied by ExxonMobil Chemical Company. It had number- and weight-average molecular weights,  $M_n$  and  $M_w$ , of 41,395 and 290,621, respectively, and a polydispersity ( $M_w/M_n$ ) of 7.02. The melting temperature ( $T_m$ ) for the sample was about  $164^\circ\text{C}$  by DSC (at a heating rate of  $4^\circ\text{Cmin}^{-1}$ ). The mesomorphic i-PP was prepared as a cast film from melt extrusion on a chill roll at a temperature of  $8^\circ\text{C}$ . The estimated quenching rate was about several hundred  $^\circ\text{C}$  per min. The quenched film

sample was cut into round disks (7 mm in diameter, 0.25 mm in thickness) and sealed into copper sample-holders with Kapton films for X-ray measurements. Simultaneous SAXS and WAXD measurements were carried out at the Advanced Polymers Beamline (X27C,  $\lambda = 1.307 \text{ \AA}$ ) in the National Synchrotron Light Source (NSLS), Brookhaven National Laboratory (BNL). Two linear position-sensitive detectors (European Molecular Biological Laboratory, EMBL) were used to detect the simultaneous SAXS and WAXD signals. The sample to detector distance for SAXS was 1590 mm, and for WAXD detection was 110 mm. The scattering data from silver behenate was used to calibrate the SAXS profile, and a mica standard from NIST was used to calibrate the WAXD profile. The heating experiments were performed using a high temperature apparatus, which has been previously described [33]. The sample was heated from 30 to  $190^\circ\text{C}$  at a rate of  $4^\circ\text{Cmin}^{-1}$  and time-resolved simultaneous SAXS and WAXD measurements were performed during this process with a data acquisition time of 30 s per scan. DSC experiments were carried out with ca. 10 mg of sample in a Perkin Elmer DSC-7 under a nitrogen purge at a rate of  $4^\circ\text{C min}^{-1}$ . The temperature and heat flow were calibrated using Indium and Tin standards.

The sample preparation scheme for transmission electron microscopy (TEM) is as follows. Along the MD–ND plane of the sample (thickness was 0.25 mm), TEM specimens were cryofaced (at  $-30^\circ\text{C}$ ) to produce a deformation-free surface using a glass knife in a cryogenic ultramicrotome (Reichert Ultracut E w/FC4D cryostage).  $\text{RuO}_4$  staining solution was prepared by adding 1 ml of NaOCl (10% wt/vol from Aldrich) to 0.02 g  $\text{RuCl}_3 \cdot n\text{H}_2\text{O}$  in a 5 ml vial, mixing well and capping immediately. The cryogenically faced samples were stained in the vapor space above the  $\text{RuO}_4$  solution for 7 h, followed by degassing in a hood for several hours. Ultra-thin sections ( $\sim 700\text{--}750 \text{ \AA}$ ) were cut at ambient temperature using a diamond knife and water floatation bath. Sections were collected onto 200 mesh carbon-coated formvar grids. Images were acquired using the JEOL 2000FX TEM (at 160 kV) and Gatan MSC-794 CCD digital camera.

## 3. Results and discussion

Typical TEM micrographs of the initial quenched i-PP sample is shown in Fig. 1a and b. In these two micrographs, ‘cluster-like’ structures with an average size of  $\sim 100 \text{ \AA}$  are visible, which fill up the entire space. The cluster size has a notably broad distribution with some having dimensions much less than  $100 \text{ \AA}$ . Such cluster structures have been reported before [34]. The crystallinity of these clusters, if any, is extremely low. A random two-phase like structure is clear in these pictures. The darker, more heavily stained regions represent the amorphous phase with no long range ordering. In contrast, the lighter, less stained regions must

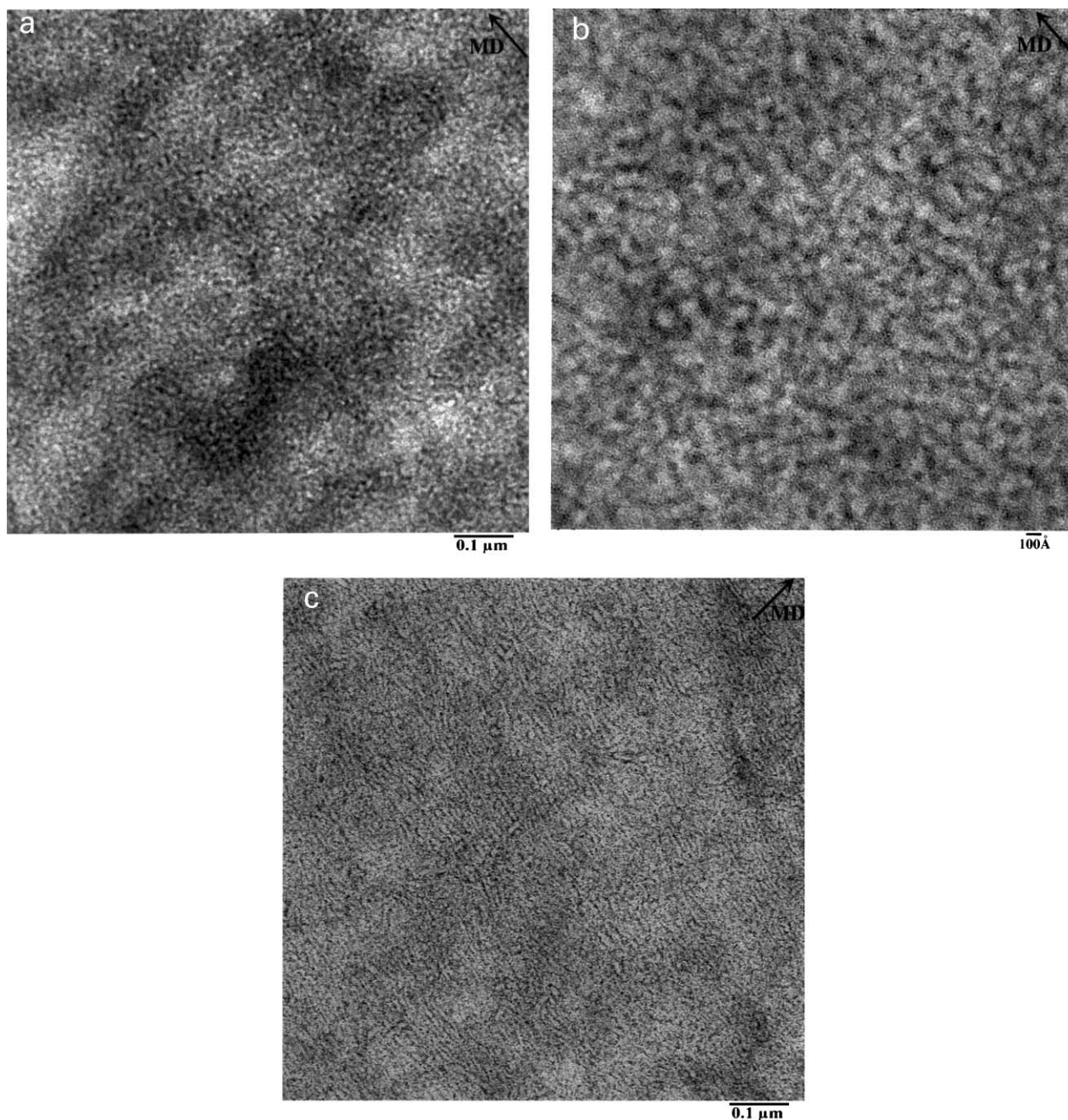


Fig. 1. Transmission electron micrograph of the etched i-PP from (a) and (b), initial mesomorphic phase with different scales; (c) annealing at 100°C for 1 h with a scale bar of 0.1  $\mu\text{m}$ .

represent the mesophase that contains some degree of ordering, resulting in a higher density less susceptible to  $\text{RuO}_4$  staining. As the chosen i-PP is known to contain a distribution of tacticity defects, it is conceivable that the clusters may be initiated from the region of high isotacticity in iPP (this would be the analog of sPP having different thermal stability in a single lamellar crystal due to the tacticity variation in the chains [35]).

The size, shape and corresponding crystal structure of the clusters are found to change quite drastically upon annealing of the sample at temperatures above 80°C. For example,

after isothermally annealing the quenched sample at 100°C for 1 h, the TEM micrograph clearly shows lamellar structures (Fig. 1c). The corresponding WAXD profile indicated that the annealed sample had an  $\alpha$ -monoclinic form. In Fig. 1c, the coexistence of both lamellar crystals and the clusters can be found. The short lamellae appear to be resulted from the aggregation of several cluster domains. Numerous lamellae with length up to  $\sim 1000$  Å are seen. The thickness of the lamellae in the annealed i-PP sample is slightly larger than the diameter of the clusters. The lamellar thickness distribution also becomes more uniform

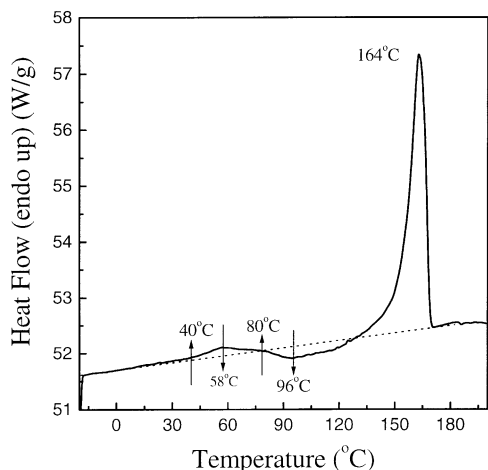


Fig. 2. DSC thermogram of i-PP film at a heating rate of  $4^{\circ}\text{C min}^{-1}$ .

than the cluster size distribution. The most interesting observation is that the lamellar orientation, to a large extent, is uniform over the whole field of view. This observation favors the conventional growth process via secondary nucleation rather than the connection of adjacent clusters, which would exhibit a more randomly arranged lamellar structure. These observations are not quite consistent with the multi-step model proposed by Strobl [6–9], since it appears that large chain reorganization has occurred before and during the transformation of mesomorphic phase to  $\alpha$ -monoclinic crystals.

Fig. 2 shows the DSC scan obtained from the quenched mesomorphic i-PP sample at a heating rate of  $4^{\circ}\text{C min}^{-1}$ . Three prominent transition peaks (a small endotherm, followed by a small exotherm and a sharp endotherm at  $164^{\circ}\text{C}$ ) are seen in the scan. The first endotherm, between  $40$  and  $80^{\circ}\text{C}$  (peak position at  $58^{\circ}\text{C}$ ), is very consistent with the chain reorganization (or ‘melting’) process in the mesomorphic phase. The broad exothermic event, between  $80$  and  $127^{\circ}\text{C}$  (center position at  $96^{\circ}\text{C}$ ), corresponds to the crystallization process to form the  $\alpha$ -monoclinic phase. The third peak, between  $127$  and  $172^{\circ}\text{C}$  (peak position at  $164^{\circ}\text{C}$ ), corresponds to the melting of the  $\alpha$ -monoclinic crystals. In this DSC scan, the true magnitude of the heat flow related to the first two transitions might be larger than the apparent value detected. This is because the net DSC scan may be due to a superposition of two large transitions with opposite signs occurring almost simultaneously, cancelling each other’s contributions.

Fig. 3a and b show selected patterns of SAXS and WAXD during heating (at a rate of  $4^{\circ}\text{C min}^{-1}$ ), respectively. For SAXS, the Lorentz-corrected intensity profiles ( $Iq^2$ ) versus scattering sector  $q$  ( $= (4\pi/\lambda)\sin(\theta)$ ,  $2\theta$  is the scattering angle) at different temperatures are shown. It is seen that there is a broad peak in the mesomorphic sample. The peak position is located at about  $0.06 \text{ \AA}^{-1}$ , which corresponds to a Bragg spacing of  $105 \text{ \AA}$ . This Bragg spacing is in good agreement with the average adjacent spacing of the clusters

observed by TEM. During heating, the Bragg spacing is nearly constant until the temperature reaches  $82^{\circ}\text{C}$ . At  $82^{\circ}\text{C}$ , the SAXS peak shifts to a lower  $q$  value ( $0.054 \text{ \AA}^{-1}$ ), corresponding to a larger spacing of  $116 \text{ \AA}$ . At  $108^{\circ}\text{C}$ , the peak  $q$  value becomes  $0.049 \text{ \AA}^{-1}$  with a corresponding spacing of  $128 \text{ \AA}$ . In addition, a broad second-order scattering peak also appears at temperatures higher than  $82^{\circ}\text{C}$ . The corresponding WAXD profiles show a similar change in phase transition (Fig. 3b). Two broad reflection peaks ( $2\theta = 15.7$  and  $20.6^{\circ}$ ) are observed for the mesomorphic phase. At  $82^{\circ}\text{C}$ , there is clear indication of a new reflection developing at  $2\theta$  of  $14.8^{\circ}$ , which represents the (110) reflection of the  $\alpha$ -monoclinic phase. This peak (marked by an asterisk at  $82^{\circ}\text{C}$ ) becomes more distinct with increase in temperature. Because the WAXD profiles have a low signal to noise ratio, we cannot deconvolute the amorphous, mesomorphic and crystal phases with good confidence. However, the identification of the phase transformation from the mesomorphic phase to the monoclinic phase can be clearly marked by following the occurrence of the peak at  $14.8^{\circ}$  (the  $\alpha$ -phase 110 reflection). Fig. 4 shows the changes of the SAXS Bragg spacing with temperature during heating. It is seen that the value remains constant at about  $105 \text{ \AA}$  before  $75^{\circ}\text{C}$ . A significant increase in the Bragg

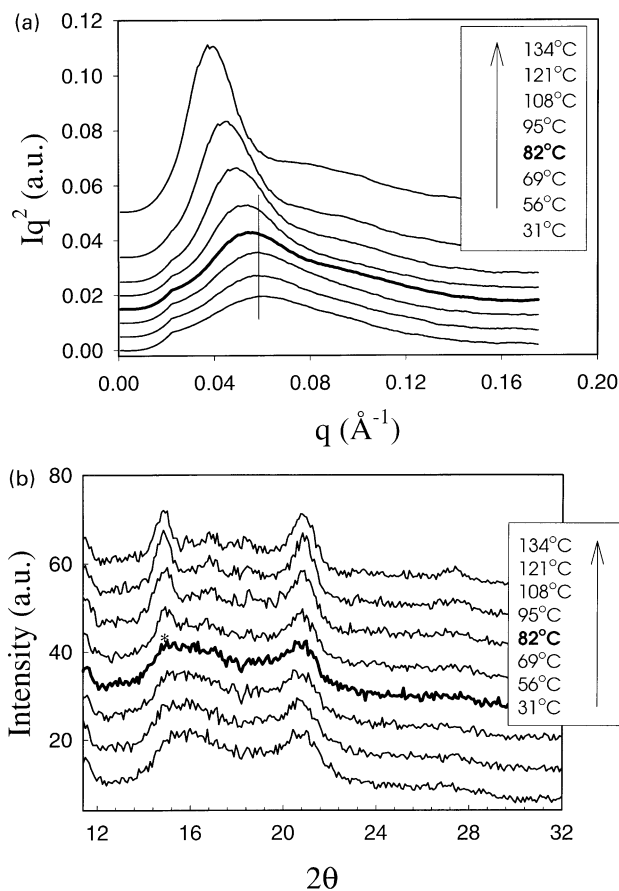


Fig. 3. Selected (a) SAXS and (b) WAXD profiles collected during heating process of i-PP at a heating rate of  $4^{\circ}\text{C min}^{-1}$ .

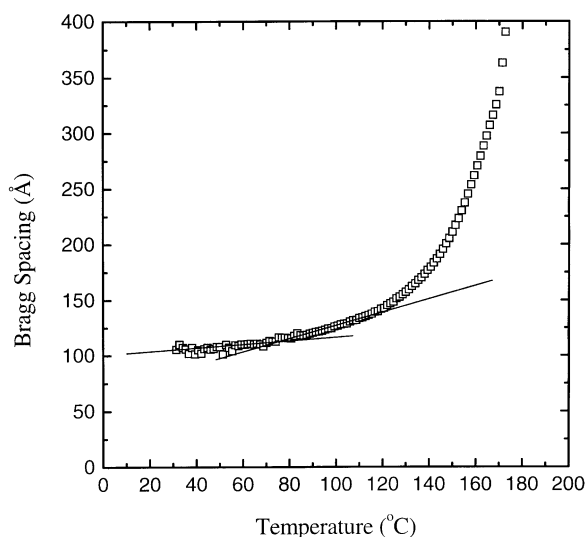


Fig. 4. Time-evolution of the Bragg spacing from the SAXS data during heating process of i-PP.

spacing occurs between 75°C ( $L_B = 115 \text{ \AA}$ ) and 127°C ( $L_B = 154 \text{ \AA}$ ), corresponding to the exothermic transition region in the DSC thermogram. At temperatures above 127°C, the Bragg spacing increases rapidly up to 380 Å, which is consistent with typical melting behavior. That is, the thinner lamellae are melted first at lower temperatures. The long period continues to increase drastically with temperature until melting of the thickest lamellae.

Based on the SAXS, WAXD, DSC and TEM results, we believe that the following mechanism is more sensible to describe the transformation of mesomorphic phase to crystal phase. As noted earlier, the mesomorphic phase represents a collection of helical chain segments with a random assembly of helical hands. Since the crystal structure of the  $\alpha$ -monoclinic phase requires specific registrations of different helical hands in the unit cell [14], the wrong adjacent helical chains in the mesomorphic phase cannot be converted into the  $\alpha$ -monoclinic phase without first correcting the helical hands. The change of the helical structure from one hand to the other requires substantial reconfiguration of the chain, which is essentially a melting process. The first endothermic event in DSC must represent the process of ‘sorting out’ the correct helical hands. During the partial melting process, the local lateral ordering of the chains may remain intact to a large degree, without causing catastrophic alteration of the global morphology. We note that there must also exist some ‘correct’ assemblies of helical chains in the cluster domains ready to form the  $\alpha$ -monoclinic structure. These assemblies thus serve as ‘primary nuclei’ for crystallization, which are ‘true precursors’ to crystallization. The subsequent crystallization step is through the secondary nucleation or conventional growth process. The continuous growth of the  $\alpha$ -monoclinic form eventually destroys the clusters, resulting in a more uniform lamellar structure. The SAXS and WAXD data show that the phase transformation occurs

over the temperature range of 75–82°C. This temperature range covers the end of the first endotherm and the onset of the exotherm by DSC. Thus, the results from SAXS, WAXD and DSC are completely consistent with each other. We notice that the i-PP chains in the mesophase become active at 40°C. In the temperature range of 40–80°C, we suggest that a significant fraction of the randomly distributed helical hands can reorganize themselves into a regular, alternating sequence of helical hands.

#### 4. Conclusions

In summary, this study indicated that the transition from mesophase to the  $\alpha$ -monoclinic crystal phase is not spontaneous, even though the initial appearance of the cluster structure in quenched mesomorphic i-PP seems to support the model of a multi-step process for crystallization in polymers [6]. The DSC heating scan, showed a small but definite low-temperature endothermic event, indicating that the chains in the mesophase underwent reorganization and converted into the crystal phase in the temperature range from 40 to 80°C. It is noted that during this temperature range, X-ray measurements (at a heating rate of  $4^\circ\text{Cmin}^{-1}$ ) cannot reveal the detailed phase transformation because of the low quantity of the  $\alpha$ -phase crystals formed and the limited detection limit of WAXD [10]. SAXS results indicate a scattering maximum (from the cluster structure) in the mesomorphic phase. The corresponding Bragg spacing maintained a constant value below 74°C, increased slowly up to 127°C (cluster to lamellar transformation), then increased rapidly until the final melting point (lamellar structure). WAXD results verified the phase transformation into the  $\alpha$ -monoclinic phase at about 80°C. We postulate that, in the cluster domains, a significant fraction of chain segments must undergo a reorganization process in order to establish the correct registration of helical hands for crystallization into the well-organized  $\alpha$ -monoclinic form. This process, which is probably through local motion of the chain segments, does not completely disrupt the local lateral ordering and the bulk morphology. A fraction of the ordered chains with correct registration of helical hands must serve as primary nuclei to initiate crystallization of the  $\alpha$ -monoclinic phase, but the entire cluster domains cannot be considered as precursors. The growth process via secondary nucleation gradually transforms the cluster structure to the lamellar structure.

#### Acknowledgements

The authors thank Dr B. Lotz for helpful insights into the crystal structures of i-PP. The financial support of this work was provided by a grant from NSF (DMR 9732653) and in part by ExxonMobil Chemical Company.

**References**

- [1] Imai M, Mori K, Mizukami T, Kaji K, Kanaya T. *Polymer* 1992;33:4451 (see also p. 4457).
- [2] Imai M, Kaji K, Kanaya T, Sakai Y. *Phys Rev B* 1995;52:12696.
- [3] Imai M, Kaji K, Kanaya T. *Macromolecules* 1994;27:7103.
- [4] Ezquerro TA, López-Cabarcos E, Hsiao BS, Baltà-Calleja F. *J Phys Rev E* 1996;54:989.
- [5] Terrill NJ, Fairclough PA, Towns-Andrews E, Komanschek BU, Young RJ, Ryan A. *J Polym* 1998;39(11):2381.
- [6] Strobl G. *Eur Phys J E: Soft Mat* 2000;3:165.
- [7] Lotz B. *Eur Phys J E: Soft Mat* 2000;3:185.
- [8] Cheng SZD. *Eur Phys J E: Soft Mat* 2000;3:195.
- [9] Muthukumar M. *Eur Phys J E: Soft Mat* 2000;3:199.
- [10] Wang ZG, Hsiao BS, Sirota EB, Agarwal P, Srinivas S. *Macromolecules* 2000;33:978.
- [11] Hauser G, Schmidtke J, Strobl G. *Macromolecules* 1998;31:6250.
- [12] Heck B, Hugel T, Iijima M, Sadiku E, Strobl G. *New J Phys* 1999;1:17.
- [13] Iijima M, Strobl G. *Macromolecules* 2000;33:5204.
- [14] Lotz B, Wittmann JC, Lovinger A. *J Polym* 1996;37:4979.
- [15] Natta G. *SPE J* 1959;15:373.
- [16] Mencik Z. *J Macromol Sci, Phys* 1972;B6(1):101.
- [17] Turner-Jones A, Cobbold AJM. *J Polym Sci* 1968;6:539.
- [18] Meille SV, Bruckner S, Porzio W. *Macromolecules* 1990;23:4114.
- [19] Natta G, Corradini P. *Nuovo Cimento Suppl* 1960;15:40.
- [20] Hsu CC, Geil PH, Miyaji H, Asai K. *J Polym Sci Polym Phys* 1986;24:2379.
- [21] Miller RL. *Polymer* 1960;1:135.
- [22] Hosemann R, Wilke W. *Makromol Chem* 1968;118:230.
- [23] Gailey JA, Ralston RH. *SPE Trans* 1964;4:29.
- [24] Bodor G, Grell M, Kallo A. *Faserforsch TextilTech* 1964;15:527.
- [25] Caldas G, Brown GR, Nohr RS, MacDonald JG, Raboin LE. *Polymer* 1994;35:899.
- [26] Murthy NS, Minor H, Bednarczyk C, Krimm S. *Macromolecules* 1993;26:1712.
- [27] Ferrero A, Ferracini E, Mazzavillani A, Malta V. *J Macromol Sci Phys* 2000;B39:109.
- [28] McAllister PB, Carter TJ, Hinde RM. *J Polym Sci, Polym Phys Edn* 1978;16:47.
- [29] Guerra G, Petraccone V, De Rosa C, Corradini P. *Makromol Chem Rapid Commun* 1985;6:573.
- [30] Corradini P, Petraccone V, De Rosa C, Guerra G. *Macromolecules* 1986;19:2699.
- [31] Corradini P, De Rosa C, Guerra G, Petraccone V. *Polym Commun* 1989;30:281.
- [32] Grebowicz J, Lau JF, Wunderlich B. *J Polym Sci, Polym Symp* 1984;71:19.
- [33] Hsiao BS, Gardner KH, Wu DQ, Chu B. *Polymer* 1993;34:3996.
- [34] Grubb DT, Yoon DY. *Polym Commun* 1986;27:84.
- [35] Zhou W, Cheng SZD, Putthanarat S, Eby RK, Reneker DH, Lotz B, Magonov S, Hsieh ET, Geerts RG, Palackal SJ, Hawley GR, Welch RB. *Macromolecules* 2000;33:6861.